THE PENNSYLVANIA STATE UNIVERSITY
SCHREYER HONORS COLLEGE

DEPARTMENT OF CHEMICAL ENGINEERING

THE EFFECTS OF EXTRACELLULAR MATRIX RIGIDITY ON TGFβ-INDUCED HISTONE MODIFICATIONS AND α-SMA EXPRESSION IN MAMMARY EPITHELIAL CELLS

APOORVA ANNAMRAJU
SPRING 2018

A thesis
submitted in partial fulfillment
of the requirements
for a baccalaureate degree
in Chemical Engineering
with honors in Chemical Engineering

Reviewed and approved* by the following:

Esther Gomez
Assistant Professor of Chemical Engineering
Thesis Supervisor

Darrell Velegol
Distinguished Professor of Chemical Engineering
Honors Adviser

* Signatures are on file in the Schreyer Honors College.

ABSTRACT

In this thesis, the effects of extracellular matrix rigidity on TGFβ-induced histone modifications and α-smooth muscle actin (α-SMA) expression in mammary epithelial cells was studied. A cavitation rheology methodology for characterization of mechanical properties of polyacrylamide hydrogels began to be developed for the research group. Hydrogels of known stiffness were analyzed by this method, and the elastic modulus was calculated using two different relationships. Equation 2 (Hutchens) was found to yield a more accurate result, and gel geometry was found to have an effect on the calculated modulus. Next, mammary epithelial cells were grown on polyacrylamide hydrogel substrata that mimicked the rigidity of normal epithelial tissue (330 Pa) and cancerous breast tissue (6320 Pa). The methyltransferase inhibitor BIX-01338 was used to inhibit methylation of lysines on histones, and expression level of α-SMA, a mesenchymal marker, was quantified to determine the extent to which epithelial-mesenchymal transition (EMT) occurred in cells. TGFβ-treated cells expressed higher levels of α-SMA when not treated with BIX-01338, indicating a relationship between histone methylation and EMT. TGFβ-treated cells grown on stiffer substrata (6320 Pa) expressed higher levels of α-SMA than cells grown on softer substrata (330 Pa), suggesting that a higher extracellular matrix rigidity further induces EMT.

TABLE OF CONTENTS

LIST OF FIGURES iii

LIST OF TABLES iv

ACKNOWLEDGMENTS v

Chapter 1 Introduction 1

- Breast cancer and cancer metastasis 1
- Epithelial-mesenchymal transition 2
- Transforming growth factor beta (TGFβ) 2
- Histone modifications and EMT 3
- Tissue stiffness and Young's modulus 3
- Hydrogel characterization and cavitation rheology 4
- Purpose 4

Chapter 2 Cavitation Rheology 6

- Introduction 6
- Methods 8
  - Polyacrylamide gel preparation 8
  - Cavitation rheology procedure 9
- Results and Discussion 11

Chapter 3 Cell Culture 17

- Introduction 17
- Methods 17
  - Solution preparation 17
  - Cell culture 17
  - Glass slide preparation 18
  - Polyacrylamide gel preparation 18
  - Polyacrylamide gel activation 19
  - Cell plating and treatments 20
  - α-smooth muscle actin (α-SMA) staining 20
  - E-cadherin (E-cad) staining 21
  - Sample imaging 21
- Results and Discussion 22

Chapter 4 Conclusions and Future Work 28

REFERENCES 30

LIST OF FIGURES

Figure 1: Cavitation rheology experimental setup 9

Figure 2: Cavitation rheology results for rectangular hydrogel 11

Figure 3: Cavitation rheology results for tubular hydrogel 13

Figure 4: No critical pressure observed during cavitation rheology of tubular hydrogel 15

Figure 5: Expression of α-SMA in cells plated on glass substrata 22

Figure 6: Percentage of cells expressing α-SMA on glass substrata 23

Figure 7: Percentage of cells expressing E-cadherin on glass substrata 24

Figure 8: Expression of α-SMA in control treatments on soft (330 Pa) and stiff (6320 Pa) polyacrylamide gels 25

Figure 9: Expression of α-SMA in TGFβ-treated cells grown on soft (330 Pa) and stiff (6320 Pa) polyacrylamide gels 26

Figure 10: Percentage of TGFβ-treated cells expressing α-SMA on soft (330 Pa) and stiff (6320 Pa) gel substrata 27

LIST OF TABLES

Table 1: Polyacrylamide gel composition for cavitation rheology 8

Table 2: Inner radii of different needle gages 10

Table 3: Calculated Young's modulus for rectangular hydrogel.....12

Table 4: Calculated Young's modulus for tubular gel.....14

Table 5: Polyacrylamide gel compositions for normal and diseased tissue.....19

Table 6: Cell treatments for each sample.....20

ACKNOWLEDGMENTS

First, I would like to sincerely thank Dr. Esther Gomez for her guidance throughout my undergraduate research career. Dr. Gomez has been essential in helping me to conduct, analyze and understand the research that I have done over the last two years. Without her help, this thesis would not have been possible. Special thanks as well to Paul Blanchard, Nagma Zerin, and Gage Virgi, for helping me to learn various lab techniques.

I would also like to thank Dr. Darrell Velegol for his support as my academic advisor throughout my undergraduate career. Dr. Velegol has been a great sounding board and his advice has helped me greatly during my time at Penn State.

Finally, I would like to thank my family and friends. Their endless support, patience, and encouragement has kept me going, and I am truly grateful.

Chapter 1

Introduction

The objectives of this thesis are to develop a methodology for characterizing polyacrylamide hydrogels by cavitation rheology, and to study the effect of extracellular matrix rigidity on TGFβ-induced histone modifications and α-SMA expression in mammary epithelial cells.

Breast cancer and cancer metastasis

Breast cancer is among the most commonly diagnosed diseases for women in the United States. Cancer is characterized on the molecular level by the uncontrolled proliferation of cells, which consume nutrients from the surrounding tissue and are unable to undergo apoptosis, or programmed cell death. Cancer metastasis refers to the spreading of cancer cells from the primary tumor site to other areas of the body, where cells can settle and form new tumors. Breast cancer metastasis is generally deadlier than the primary tumor itself. The five-year relative survival rate for breast cancer patients that are treated before cancer metastasis is 98.9%; however, for patients treated after metastasis to regional lymph nodes, the five-year survival rate is 85.2%, and for those treated after metastasis to other organ systems, it is only 26.9% (National Cancer Institute).

Epithelial-mesenchymal transition

Cancer metastasis has been linked to epithelial-mesenchymal transition (EMT), a process involved in embryonic development, tissue regeneration, and wound healing (Kalluri). EMT is a molecular process in which epithelial cells undergo biochemical modifications to become mesenchymal cells, which have different physical properties. Epithelial cells have a rounded cobblestone-like shape, and they adhere to each other and to the basement membrane in order to form the lining of mammary tubules and various other organs. They are unable to migrate to other regions of the body (Angadi). Mesenchymal cells, however, have an elongated spindle shape and weak intercellular interactions. They have increased resistance to apoptosis and possess migratory capabilities (Angadi, Turley, Kalluri). Thus, when cancerous cells undergo EMT, they are able to migrate away from the primary tumor, leading to metastasis.

Transforming growth factor beta (TGFβ)

For the experiments described within this thesis, EMT was induced by transforming growth factor beta (TGFβ). TGFβ is secreted by certain immune cells, as well as by epithelial cells for epithelial tissue regulation and wound healing (Massague). In addition, TGFβ levels have been found to be elevated in the context of cancer. Moreover, TGFβ has also been found to induce EMT. It binds to receptor kinases displayed on the cell surface and can use Smad-dependent or Smad-independent signaling pathways to affect expression of other growth factors and proteins (Nalluri). Smads are proteins that when activated, translocate to the nucleus to regulate transcription of target genes (Fafet). One Smad-dependent pathway activates Snail and Slug transcriptional repressors, which causes downregulation of the epithelial protein E-cadherin

after EMT has occurred. Other pathways cause upregulation of the mesenchymal protein alpha smooth muscle actin (α-SMA) (Thierry, Angadi).

Histone modifications and EMT

Epigenetic modifications affect gene expression by changing DNA packaging or chromatin without changing the DNA sequence. For example, histones, the proteins involved in DNA packaging, can be methylated on specific amino acid residues, which can affect ease of transcription at genes located near the methylation site. Epigenetic modifications have been found to play a role in EMT (McDonald). In this thesis, the impact of methylation of histones on EMT was studied. For example, histone modification H3K36Me3, which corresponds to a trimethylation (Me3) at heterochromatin mark H3, lysine residue 36, is known to increase in response to TGFβ (McDonald). In order to study how methylation of histones affects EMT, an inhibitor called BIX-01338 was introduced to cells. BIX-01338 is a broad-spectrum methyltransferase inhibitor, which blocks methylation at H3 (Liu).

Tissue stiffness and Young's modulus

Cancer tissue has been found to have greater stiffness than normal tissue in that area of the body. Normal breast tissue has a stiffness of ~150 Pa, while breast cancer tissue has a stiffness of ~1500-5000 Pa (Cox). Matrix rigidity has been found to have an effect on the extent to which EMT occurs (O'Connor). This thesis examines the effects of matrix rigidity on the expression of α-SMA during TGFβ-induced EMT, and whether this process is regulated by histone methylation.

Material stiffness can be described quantitatively using the Young's modulus, which refers to the resistance of the material to a stress. Mathematically, it is the force applied per unit area, or tensile stress, divided by the relative change in length, or the resulting strain (Discher, Tse). Tissues in various parts of the body have unique elastic moduli, which can be mimicked *in vitro* using hydrogels with corresponding moduli (Tse). In this thesis, the mechanical properties of normal and diseased mammary tissue are mimicked using polyacrylamide hydrogels.

Hydrogel characterization and cavitation rheology

There are a few methods that can be used to determine the modulus, or stiffness, of a soft material, such as parallel plate rheometry and atomic force microscopy (AFM). However, these methods can be expensive, and they often require large quantities of the material being characterized (Zimberlin). Additionally, material heterogeneities cannot be detected by parallel plate rheometry.

Cavitation rheology is a technique by which the local modulus of a soft material can be determined by injecting a needle into the material at a specified location and inducing a bubble to form by injecting air. In this thesis, a methodology for using cavitation rheology to characterize hydrogels for cell culture began to be developed for the research group.

Purpose

The purpose this thesis is to determine how extracellular matrix rigidity affects TGFβ-induced histone modifications and α-SMA expression in mammary epithelial cells. First, a cavitation rheology methodology will be developed for use within the research group. Then, cell

culture experiments will be conducted. Expression of α-SMA, a mesenchymal marker, will be quantified to determine the extent to which EMT has occurred. It is hypothesized that α-SMA expression will be greater in samples treated with TGFβ on a stiffer matrix. It is also hypothesized that samples treated with the methyltransferase inhibitor BIX-01338 and TGFβ will have less expression of α-SMA than those only treated with TGFβ, because BIX-01338 inhibits methylation of histone H3. Histone methylation is believed to be important for the regulation of α-SMA expression during EMT.

Chapter 2

Cavitation Rheology

Introduction

Cavitation rheology is a method by which the local modulus of a soft material can be quantified. For this method, an air bubble is injected into the material using a needle attached to a syringe pump. The pressure inside the cavity is monitored until the cavity bursts, indicating mechanical instability (Kundu). The pressure at this point is called the critical pressure (P_c), and it can be related to the local modulus (E) by the linear relationship in Equation 1, where γ is the surface energy and r is the inner radius of the needle.

$$P_c = \frac{2\gamma}{r} + \frac{5}{6}E \quad \text{(Eq. 1)}$$

The relationship in Equation 1 is derived from a simplified strain-energy function for an incompressible neo-Hookean material such as a hydrogel (Zimberlin). However, this method assumes that the shape of the cavity induced is spherical (Hutchens). A later study of this method determined that the shape of the cavity induced into a polyacrylamide hydrogel is actually a spherical cap, thus changing the relationship between critical pressure and elastic modulus, as shown in Equation 2 (Hutchens). In this thesis, both Equations 1 and 2 are used to evaluate the modulus determined by cavitation rheology of a material with a known modulus, in order to determine which is more appropriate for the polyacrylamide hydrogels used.

$$P_c = \frac{2.1\gamma}{r} + 1.05E \quad \text{(Eq. 2)}$$

Cavitation rheology could potentially be used to quantify the stiffness of a hydrogel scaffold without disrupting cell growth. Thus, gels could be charaterized while cells are growing on them to determine if EMT or other cell changes have an impact on the matrix stiffness. Cavitation rheology is also an advantageous method to be used with a dynamic scaffold. A dynamic hydrogel would have the ability to decrease or increase in stiffness over time, so epithelial and cancerous cells grown on this matrix can be observed as the extracellular environment undergoes changes in rigidity.

In this thesis, a cavitation rheology instrument was set up, and it was tested using hydrogels with known mechanical properties.

Methods

Polyacrylamide gel preparation

Polyacrylamide (PA) gel solution was prepared to achieve a stiffness of 1800 ± 440 Pa when polymerized (Tse). The gel composition can be seen in Table 1.

Table 1: Polyacrylamide gel composition for cavitation rheology

% acrylamide	% bis-acrylamide	Volume acrylamide (µL)	Volume bis-acrylamide (µL)	Volume dH_2O (µL)
5	0.06	125	30	839.5

Acrylamide, bis-acrylamide, and dH_2O were combined at desired concentrations and placed in the desiccator to degas for 30 minutes. Gel polymerization was initiated by adding 0.5 µL tetramethylethylenediamine (TEMED) and 5 µL 10% (w/v) ammonium persulfate (APS) to the solution and mixing thoroughly. Two different geometries of hydrogels were used for this thesis:

Rectangular geometry: 850 µL of solution was added to the center of a 22 mm x 40 mm glass slide, and another 22 mm x 40 mm slide was gently placed on top of the solution. Polymerization occurred in 1-2 hours.

Tube geometry: The gel solution was divided into 600 µL batches and left in Eppendorf tubes to polymerize. Tubes were used so that the needle injection depth could be measured and kept at a constant value of 2 mm.

After polymerization, gels were covered in 1× PBS and stored in the 4 °C refrigerator until used.

The modulus for a gel containing 5% acrylamide and 0.06% bis-acrylamide is ~1800 Pa, according to AFM experiments (Tse). However, parallel plate rheometry experiments previously performed in the Gomez lab have determined a modulus of ~4600 Pa for this gel composition.

Cavitation rheology procedure

The cavitation rheology instrument consists of the following parts: a syringe pump, a pressure transducer, a stage, and needles of various gauges. The experimental setup can be seen in Figure 1. The computer programs used were SyringePumpPro and a custom Labview program written to run the instrument and record the pressure as a function of time.

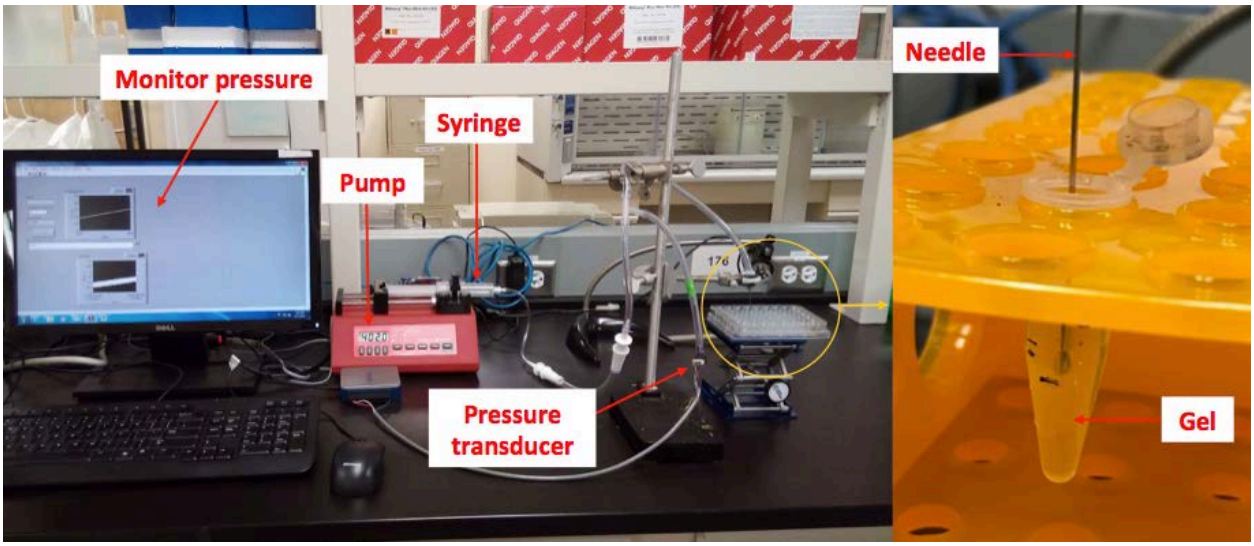

Figure 1: Cavitation rheology experimental setup
Left: Syringe pumps air through the tubing, where the pressure transducer detects gauge pressure, which is recorded in the custom Labview computer program. **Right:** Needle is injected orthogonally into the gel, and the air pumped by the syringe introduces a bubble into the gel.

PA gels were brought to room temperature. A needle was attached to the instrument and clamped such that the needle position was orthogonal to the bench surface. For the tubular gels, he Eppendorf tube was marked at the gel surface and at 2 mm below the surface to ensure that the needle insertion depth was consistent. The tube was placed on a stage beneath the needle and was oriented such that the needle would not touch the inner tube wall when inserted into the gel. The stage was slowly moved upward until the needle had pierced the gel to the mark made previously. The LabView cavitation rheology program and syringe pump were started. The program was run until a pressure drop (cavitation peak) was observed. The pump was then stopped and the stage was slowly lowered until the needle was fully removed from the hydrogel. This procedure was run three times, each using a different needle gage (Table 2).

Table 2: Inner radii of different needle gages

Needle gage	Inner radius (mm)
22	0.413
25	0.260
30	0.159

The pressure versus time data for each run was graphed. The critical pressure was determined by finding the maximum pressure change during the run. Critical pressure was then graphed as a function of the inverse of the inner needle radius (mm^{-1}). Young's modulus (E) was calculated twice, using the relationships described in Equations 1 and 2.

Results and Discussion

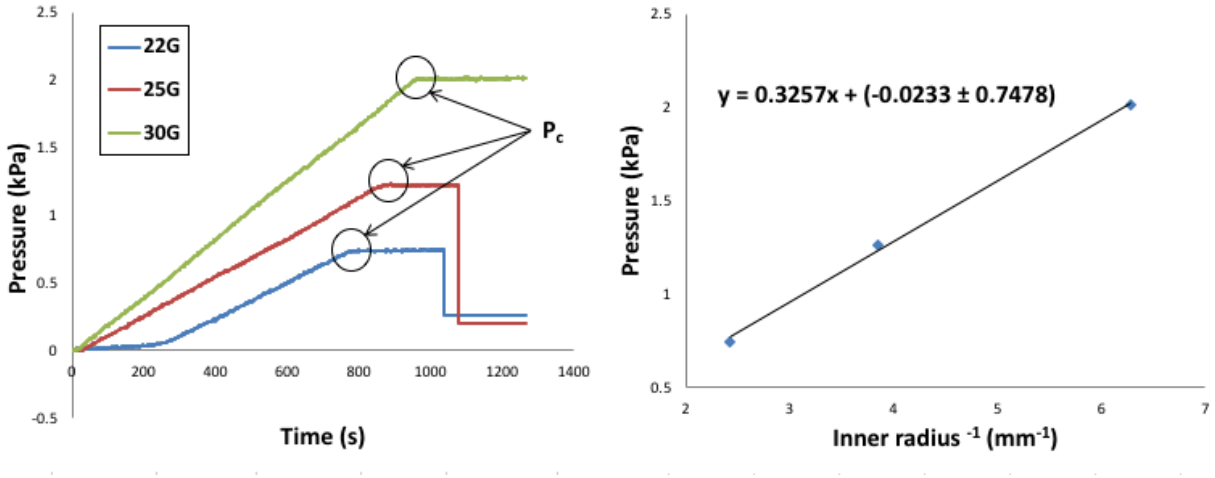

Figure 2: Cavitation rheology results for rectangular hydrogel
Left: Pressure versus time profiles for cavitation using three needle gages (22G, 25G, 30G) with critical pressure (P_c) circled in black. **Right:** Critical pressure versus inner radius of needle, where the y-intercept (shown with 90% confidence interval) is used to calculate the local modulus (*E*).

Cavitation rheology was first used to characterize an 850 µL hydrogel with a rectangular geometry. The gel was probed at 9 different locations, where each needle gage was used to probe three different locations.

The graph to the left in Figure 2 shows a pressure versus time profile for each needle gage, where the maximum pressure (circled in black) is the critical pressure at which mechanical instability of the growing air bubble within the material is reached.

All 3 profiles show that once the maximum pressure was reached, the pressure stopped increasing and stayed constant. A sharp decrease in pressure is generally the sign that the cavity has burst. Since there was a sharp decrease in pressure for the 25-gage and 30-gage needles after about 200 seconds at a constant pressure, it was assumed that this constant pressure was the

critical pressure. The same assumption was made for the 22-gage needle profile, although the run was stopped before the pressure drop was seen.

The critical pressure increases as needle gage increases (Figure 2, left), where a higher needle gage corresponds to a smaller inner radius (Table 2). The averages of the 3 critical pressures measured for each needle gage were plotted against the inverse of the needle radius (Figure 2, right) to determine the intercept of the best-fit line. The Young's modulus of the material can be calculated by substituting the intercept of the line into the intercept expression in Equation 1 or Equation 2. The calculated elastic moduli for both equations are shown in Table 3.

Table 3: Calculated Young's modulus for rectangular hydrogel

Moduli were calculated using the relationships from Equations 1 and 2. Both moduli calculated are negative, indicating some error associated with the data collected in this experiment.

Intercept ($P_{c,0}$)	Relationship	E (Pa)
-23.3 Pa	$E = (6/5)\ P_{c,0}$	-27.96
	$E = (1/1.05)\ P_{c,0}$	-22.19

The data in Table 3 indicates that a negative modulus was obtained for the rectangular geometry. There must be some error associated with this data, since the modulus for this material should not be negative. The rectangular gel is not very thick, so the needle could have contacted the surface of the glass support instead of just the gel. Another reason for this error could be that the cavity was induced too close to the interface between the gel and the glass, causing the cavity to contact the glass and become deformed.

The next experiment was run using hydrogels with a tubular shape in order to avoid contact between the needle and the glass, and between the bubble and the glass. 600 µL of gel solution was left to polymerize in an Eppendorf tube, and a mark was made at 2 mm below the gel surface to keep the needle insertion depth constant.

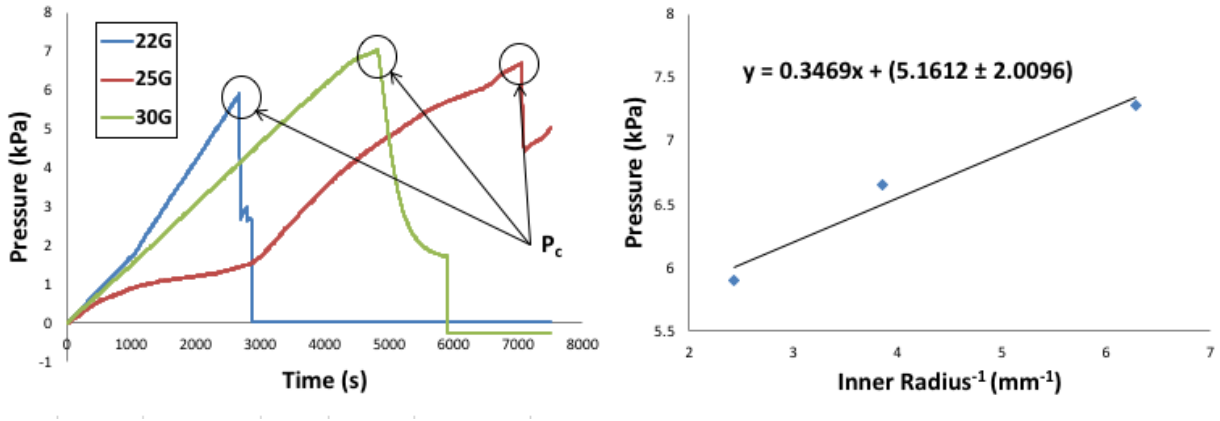

Figure 3: Cavitation rheology results for tubular hydrogel
Left: Pressure versus time profiles for cavitation using three needle gages (22G, 25G, 30G) with critical pressure (P_c) circled in black. **Right:** Critical pressure versus inner radius of needle, where the y-intercept (shown with 90% confidence interval) is used to calculate the local modulus (*E*).

Each tubular gel was probed at 6 different locations, where each needle gage was used twice. Only one trial of each needle gage showed cavitation, so only the data from these runs was used to determine the modulus of the material. The graph to the left in Figure 3 shows a pressure versus time profile for each needle gage, with the critical pressures circled in black. All three profiles showed a sharp drop in pressure after the maximum pressure was reached, indicating that the cavity collapsed. The critical pressures for the tubular hydrogel are plotted against the inverse of the needle radius (Figure 2, right). The calculated elastic moduli are shown in Table 4.

Table 4: Calculated Young's modulus for tubular gel

Moduli were calculated using the relationships from Equations 1 and 2. The modulus from the Equation 2 relationship closely resembles the modulus determined by parallel-plate rheometry, suggesting that Equation 2 is more appropriate for polyacrylamide hydrogels.

Intercept ($P_{c,0}$)	Relationship	E (Pa)
5161 Pa	$E = (6/5)\ P_{c,0}$	6193
	$E = (1/1.05)\ P_{c,0}$	4915

The data in Table 4 shows a difference between the moduli obtained from Equations 1 and 2 and the expected modulus from AFM experiments (1800 Pa). However, the modulus obtained using Equation 2 (4915 Pa), is within 6.8% of the modulus obtained for this gel composition by parallel plate rheometry (4600 Pa), suggesting that Equation 2 is a more appropriate model to describe this system. This is consistent with reports by Hutchens showing that Equation 2 is most appropriate for analysis of polyacrylamide hydrogels, due to the geometry of the cavity formed.

The time it took to achieve cavitation varied significantly between the two geometries. The rectangular hydrogel showed cavitation at 800-1000 seconds (Figure 2, left), while the tubular hydrogel showed cavitation at 3000-7500 seconds (Figure 3, left). This difference can be partially attributed to inconsistencies in needle depth or contact with the underlying surface in the rectangular gel geometry. However, this could also suggest that the gel geometry or the needle insertion depth have an effect on the time required for cavitation.

There were some inconsistencies in the data collection using the cavitation rheology approach, particularly for the tubular geometry. While the same protocol was followed for every trial, different results were obtained for the critical pressure, and the shape of the pressure versus

time profile changed. Some trials did not show a cavitation peak at all; the pressure just continued increasing (Figure 4). In cases such as the trial shown in Figure 4, the needle was usually either clogged, or too close to the inner wall of the Eppendorf tube containing the gel. To resolve these issues, the needle was replaced and the injection site was changed.

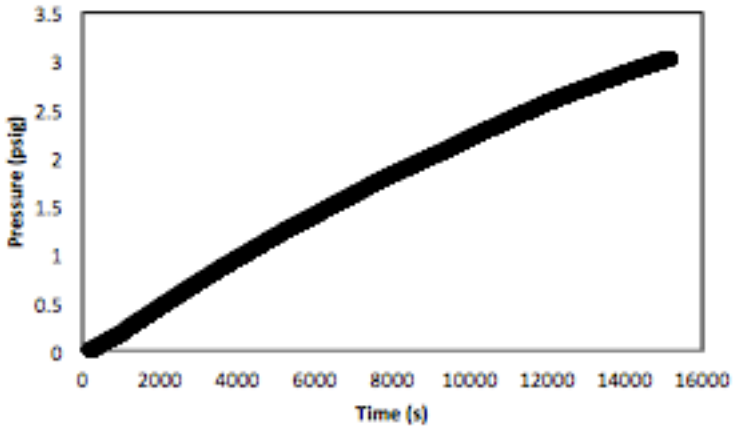

Figure 4: No critical pressure observed during cavitation rheology of tubular hydrogel

There are several other potential reasons for experimental error. The hydrogels could have not polymerized evenly, despite the mixing of the solution with the polymerization initiators when the gel solution was first prepared. This would explain the different results obtained for different locations probed within the same sample. For future experiments, the gel solution may need to be mixed using a vortex mixer instead of a pipette. Additionally, physical observations during the runs showed that bubbles formed in the gel but were not detected by the software at times. If cavitation was occurring much earlier than indicated by the program, then the gel could have been damaged, which could then affect the accuracy of the critical pressure determined. To resolve this issue, different tubing or a new pressure transducer should be used to ensure accurate pressure readings.

Overall, the results obtained from the cavitation rheology instrument were inconsistent. While the set up yielded an accurate local modulus value when using a tubular hydrogel, the data was not able to be reproduced. Further work should be done with this set up to ensure that the data collected is accurate and reproducible.

Chapter 3

Cell Culture

Introduction

The histone modification H3K36Me3 has been found to increase in response to TGFβ (McDonald). Thus, we sought to determine if methylation of histones regulates aspects of EMT. This was studied by introducing BIX-01338, a methyltransferase inhibitor, to cells treated with and without TGFβ. Expression of alpha smooth muscle actin (α-SMA), a mesenchymal marker, was quantified to determine the extent to which EMT occurred for each cell treatment.

Methods

Solution preparation

First, solutions were prepared for these experiments. 1× phosphate-buffered saline (PBS) was utilized as a buffer for several experimental methods. It was prepared by dilution of 10× PBS with deionized water (dH_2O).

Cell culture

Normal murine mammary gland (NMuMG) epithelial cells were cultured in DMEM media containing 10% fetal bovine serum (FBS), 0.1% gentamicin and 0.1% insulin.

Glass slide preparation

22×22 mm glass slides were used as substrata for cell culture for some experiments. Slides were sterilized by incubation in ethanol for 5 minutes and left to dry. Slides were then placed in individual wells of a 6-well plate and covered with 150 µL each of 25 µg/mL human plasma fibronectin diluted in sterile 1× PBS. Slides were then left overnight in the 4 °C refrigerator. Slides were rinsed thoroughly with PBS to remove excess fibronectin. Slides were covered in PBS and stored in the 4 °C refrigerator until used.

Polyacrylamide gel preparation

22 mm × 22 mm glass slides were incubated in 0.1 N NaOH for 15 minutes. Slides were rinsed thoroughly with dH_2O and dried completely. Slides were then incubated in 2% (v/v) aminopropyl trimethoxysilane (APTMS) diluted in acetone for 15-30 minutes. Slides were rinsed thoroughly with acetone and left to air dry. Then, slides were incubated in 0.5% glutaraldehyde diluted in 1× PBS for 30 minutes. Slides were thoroughly rinsed with dH_2O and dried completely.

Circular 22 mm glass slides were treated with Rain-X by wiping slides with Rain-X, leaving them until cloudy, and then wiping slides until no longer cloudy.

Polyacrylamide (PA) gel solutions were prepared to achieve two different stiffnesses when polymerized: 330 Pa and 6320 Pa. Gel compositions can be seen in Table 2.

Table 5: Polyacrylamide gel compositions for normal and diseased tissue

Stiffness (Pa)	% acrylamide	% bis-acrylamide	Volume acrylamide (μL)	Volume bis-acrylamide (μL)	Volume dH_2O (μL)
330	5	0.015	125	7.5	862
6320	7.5	0.2	187.5	100	707

Acrylamide, bis-acrylamide, and dH_2O were combined at desired concentrations and placed in the desiccator to degas for 30 minutes. Gel polymerization was initiated by adding 0.5 μL tetramethylethylenediamine (TEMED) and 5 μL 10% (w/v) ammonium persulfate (APS) to the solution and mixing thoroughly. 20 μL of solution was added to the center of each prepared square slide, and a Rain-X treated circular slide was placed on top of the solution. Polymerization occurred in 30-45 minutes. After polymerization, gels were placed in 1× PBS and stored in the 4 °C refrigerator until activated.

Polyacrylamide gel activation

Gels were removed from 1× PBS. 200 μL of 0.25 mg/mL Sulfo-SANPAH in HEPES (4-(2-hydroxyethyl)-1-piperazineethanesulfonic acid) buffer solution (pH 8.5) was added on top of each gel, and gels were placed in the CL-1000 Ultraviolet Crosslinker for 10 minutes. Sulfo-SANPAH was then removed from gels, and gels were rinsed with HEPES. 200 μL Sulfo-SANPAH was added to gels again, and they were placed in the UV Crosslinker for 10 minutes.

Gels were then moved to a sterile biosafety hood and rinsed with sterile HEPES. 200 μL of 25 μg/mL human plasma fibronectin diluted in sterile HEPES was added to each gel. Gels

were then left overnight in the 4 °C refrigerator. Gels were rinsed with sterile 1× PBS and then sterilized by incubation in 70% ethanol for 30 minutes. Ethanol was aspirated off, and gels were rinsed with sterile 1× PBS.

Cell plating and treatments

Cells were plated at 50,000 cells/well on treated glass slides, or at 150,000 cells/well on polyacrylamide gels. Cells were left to incubate overnight to allow for the cells to adhere to the substrate. Cells were then initiated with treatments. Half of the samples were treated with 10 ng/mL TGFβ, and samples were treated with either 1.67 nM BIX-01338 or 1.67 nM DMSO (dimethyl sulfoxide). Cells were left to incubate for 48 hours. See Table 6 for cell treatments.

Table 6: Cell treatments for each sample

	Control	**TGFβ**
DMSO	Cell Treatment 1	Cell Treatment 3
BIX	Cell Treatment 2	Cell Treatment 4

α-smooth muscle actin (α-SMA) staining

Cells were fixed with 1:1 methanol/acetone at -20 °C for 10 minutes and rinsed thoroughly with 1× PBS. Cells were blocked with 10% goat serum and 0.1% Tween in 1× PBS and incubated with primary antibodies (mouse-anti-α-SMA diluted 1:200 in blocking buffer). Samples were rinsed with 1× PBS and incubated with secondary antibodies (goat-anti-mouse

Alexa 594 diluted 1:500 in blocking buffer). Cell nuclei were also stained with Hoechst 33342 (1:10000 dilution) in 1× PBS.

E-cadherin (E-cad) staining

Cells were fixed with 4% formaldehyde diluted in 1× PBS and rinsed thoroughly with PBS. Cells were blocked with 5% goat serum and 0.3% Triton X-100 in 1× PBS and incubated with primary antibodies (rabbit-anti-E-cadherin diluted in 1% BSA and 0.3% Triton X-100 in 1× PBS). Samples were rinsed with PBS and incubated with secondary antibodies (goat-anti-rabbit Alexa 594 diluted 1:500 in primary antibody dilution buffer). Cell nuclei were also stained with Hoechst 33342 (1:10000 dilution) in 1× PBS.

Sample imaging

Stained samples were imaged using a Nikon Eclipse Ti-E fluorescence microscope with a 20× air objective. Images were analyzed using ImageJ software to determine the percentage of cells expressing α-SMA.

Results and Discussion

Cells were plated on glass substrata first in order to study and quantify expression of α-SMA in cells treated with TGFβ and either BIX or DMSO. DMSO was used as a control for the BIX treatment, since the BIX-01338 stock solution used was diluted in DMSO.

α-SMA levels were found to increase in cells treated with TGFβ compared to those not treated with TGFβ. Cells treated with TGFβ and BIX were observed to have lower α-SMA levels than cells treated with TGFβ and DMSO.

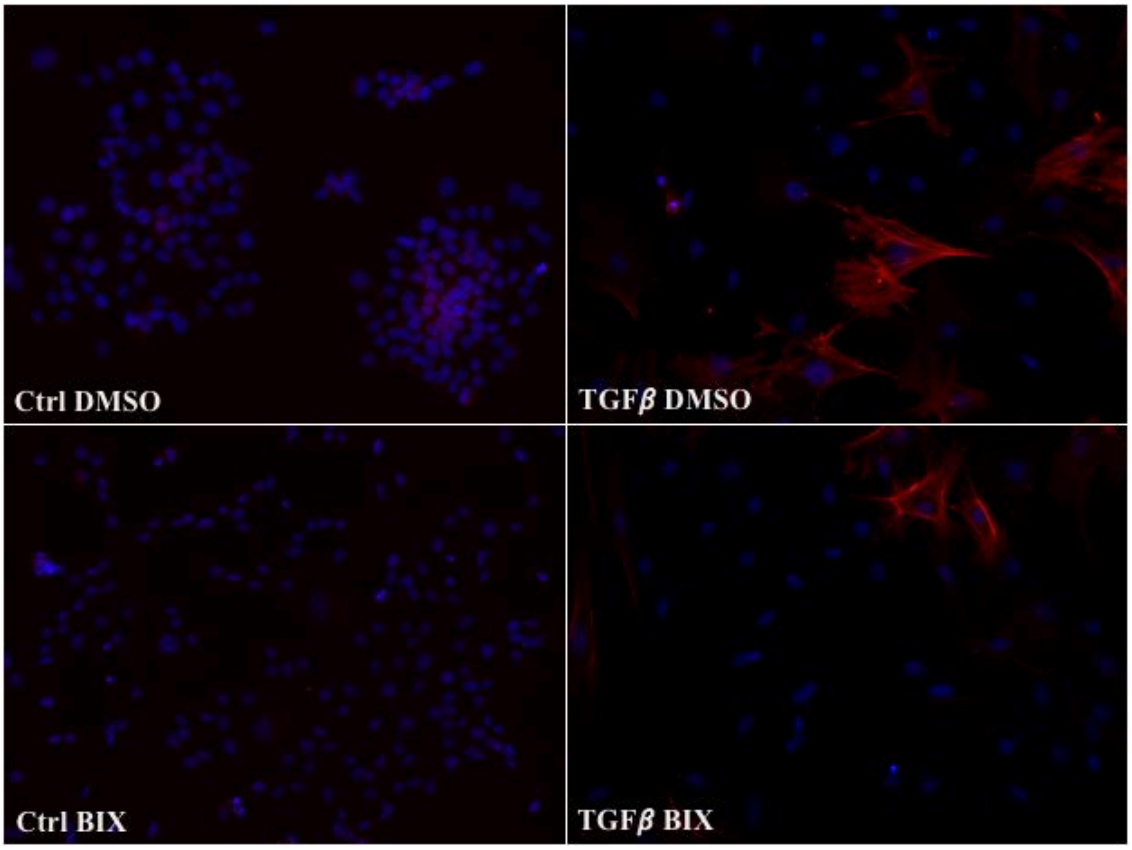

Figure 5: Expression of α-SMA in cells plated on glass substrata
α-SMA (shown as red fibers) is not expressed in non-TGFβ treated cells (Ctrl DMSO, Ctrl BIX), and is expressed more for TGFβ DMSO treatment than TGFβ BIX treatment. Cell nuclei are shown in blue.

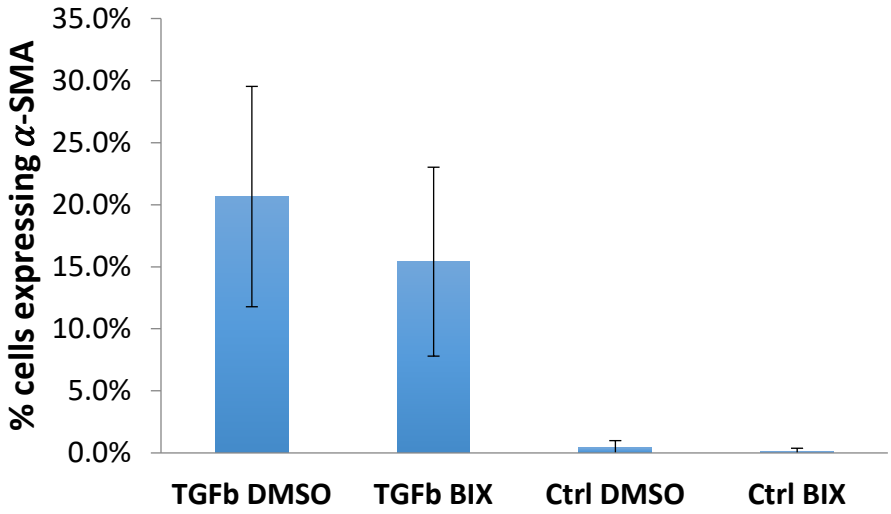

Figure 6: Percentage of cells expressing α-SMA on glass substrata
Non-TGFβ treated cells (Ctrl DMSO, Ctrl BIX) express little to no α-SMA. A larger percentage of cells treated with TGFβ and DMSO express α-SMA than cells treated with TGFβ and BIX.

Figure 5 shows α-SMA stained in red, and the cell nuclei stained in blue. As shown in Figures 5 and 6, cells not treated with TGFβ had little to no expression of α-SMA. This is to be expected, since α-SMA is a mesenchymal cell marker, and the cells not treated with TGFβ would not have undergone EMT. However, these cells do have higher levels of E-cadherin, an epithelial cell marker, while the cells treated with TGFβ show little to no expression of E-cadherin (Figure 7). The relative levels of α-SMA and E-cadherin confirm that the cells treated with TGFβ underwent EMT.

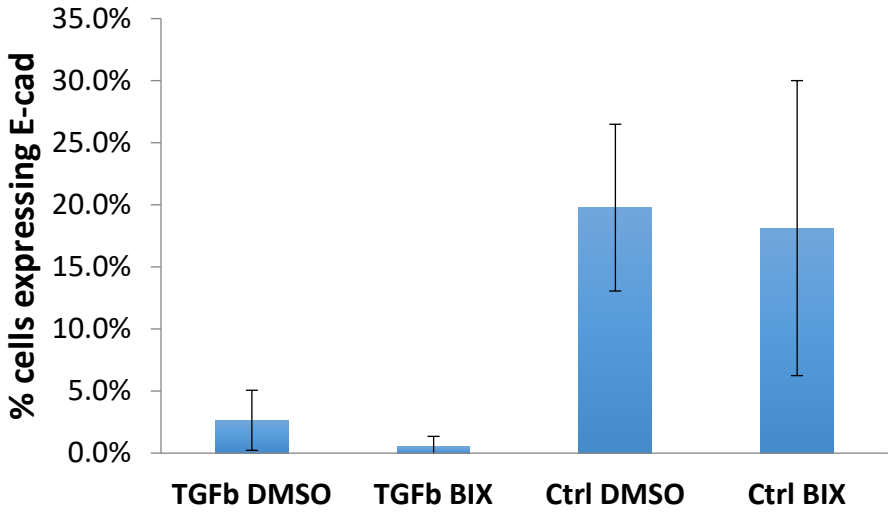

Figure 7: Percentage of cells expressing E-cadherin on glass substrata
Non-TGFβ treated cells (Ctrl DMSO, Ctrl BIX) express E-cadherin more frequently than cells treated with TGFβ.

Figures 5 and 6 also show that for the TGFβ-treated cells, those treated with BIX had lower α-SMA levels than those treated with DMSO. This shows that methylation of histones is related to EMT, since BIX-01338 inhibits the methyltransferases that add methyl groups to histones. The lower expression level of α-SMA in the presence of BIX suggests that methylation of H3K36 may contribute to EMT, which was hypothesized at the start of the experiment; however, further experiments are needed to confirm the role of this specific methylation site.

Although glass is a popular substrate for cell culture experiments, it is much more rigid than the environments in which cells grow in the body. Cells with each treatment were grown on polyacrylamide gel matrices with stiffnesses mimicking those of normal (330 Pa) and cancerous (6320 Pa) mouse mammary tissue (Lopez). Levels of α-SMA were hypothesized to be higher in cells grown on the stiffer gel matrix compared to those grown on the softer gel matrix.

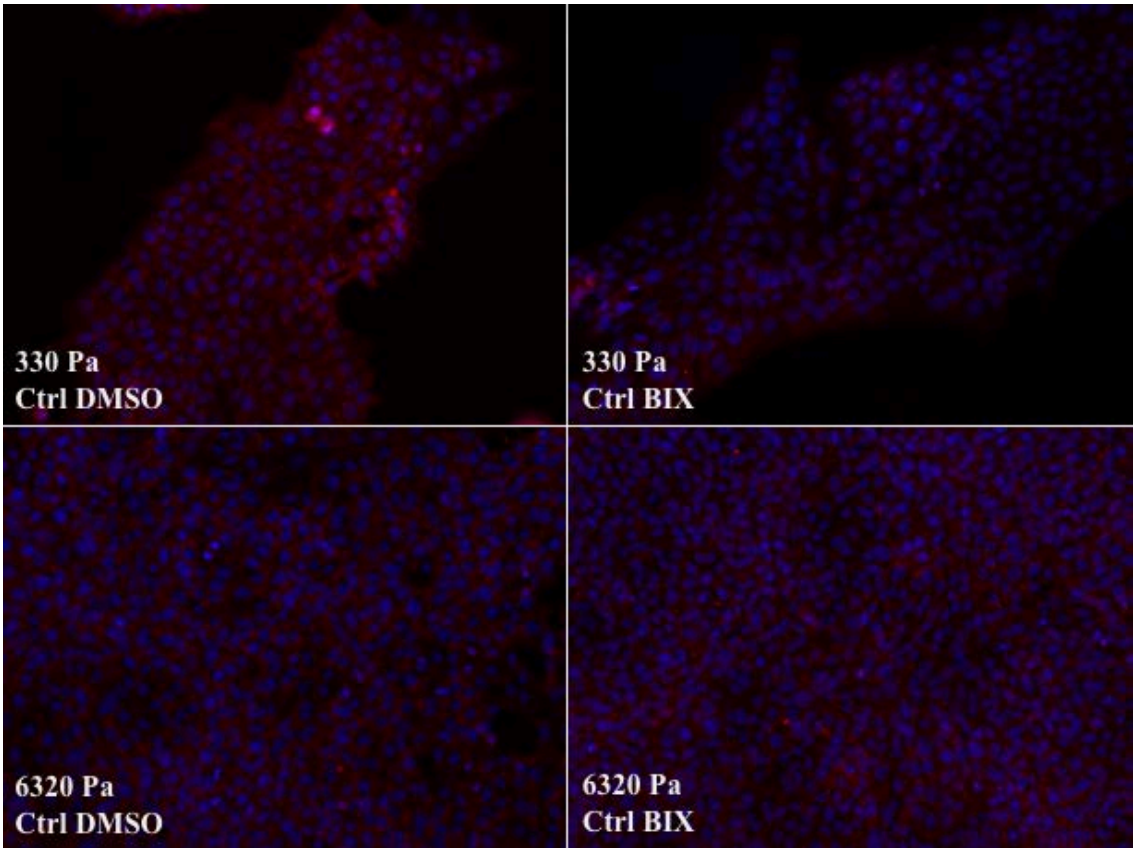

Figure 8: Expression of α-SMA in control treatments on soft (330 Pa) and stiff (6320 Pa) polyacrylamide gels

α-SMA (shown as red fibers) is not expressed in non-TGFβ treated cells (Ctrl DMSO, Ctrl BIX) grown on either a soft or stiff gel matrix. Cell nuclei are shown in blue.

Cells not treated with TGFβ did not express α-SMA (Figure 8). Again, this was expected, since α-SMA is a mesenchymal cell marker, and cells not treated with TGFβ would not have undergone EMT. The matrix stiffness had no effect on the expression of α-SMA for non-TGFβ-treated cells. However, the TGFβ-treated cells grown on a stiffer gel matrix (6320 Pa) expressed α-SMA more frequently than those grown on a softer gel matrix (330 Pa) (Figure 9).

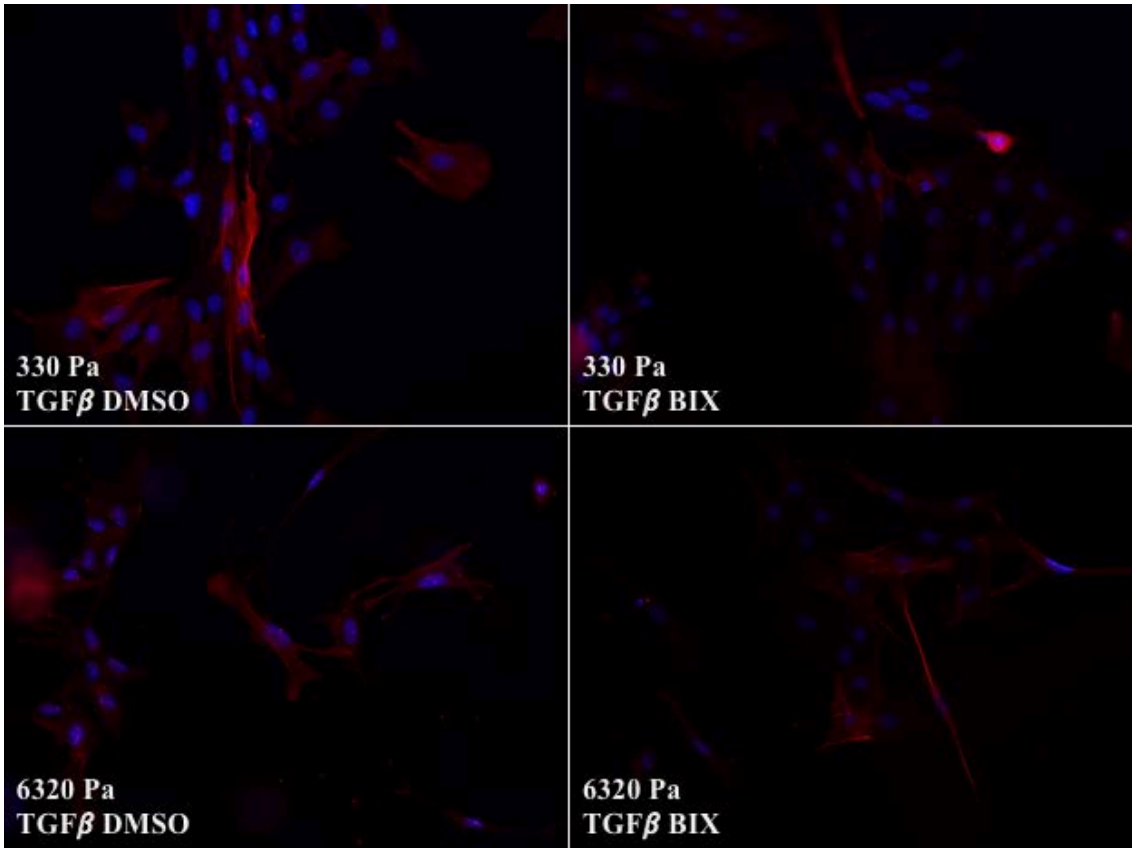

Figure 9: Expression of α-SMA in TGFβ-treated cells grown on soft (330 Pa) and stiff (6320 Pa) polyacrylamide gels

α-SMA (shown as red fibers) is expressed more for cells treated with DMSO than cells treated with BIX. α-SMA is also expressed at a higher frequency for cells grown on a stiffer gel matrix (6320 Pa) than for cells grown on a softer gel matrix (330 Pa). Cell nuclei are shown in blue.

Figures 9 and 10 show that α-SMA levels are higher in cells treated with TGFβ and DMSO than in cells treated with TGFβ and BIX. This result is consistent with the results of cells grown on glass substrata (Figures 5 and 6), further suggesting that the methylation of H3K36 may have an effect on expression of α-SMA in TGFβ-treated cells.

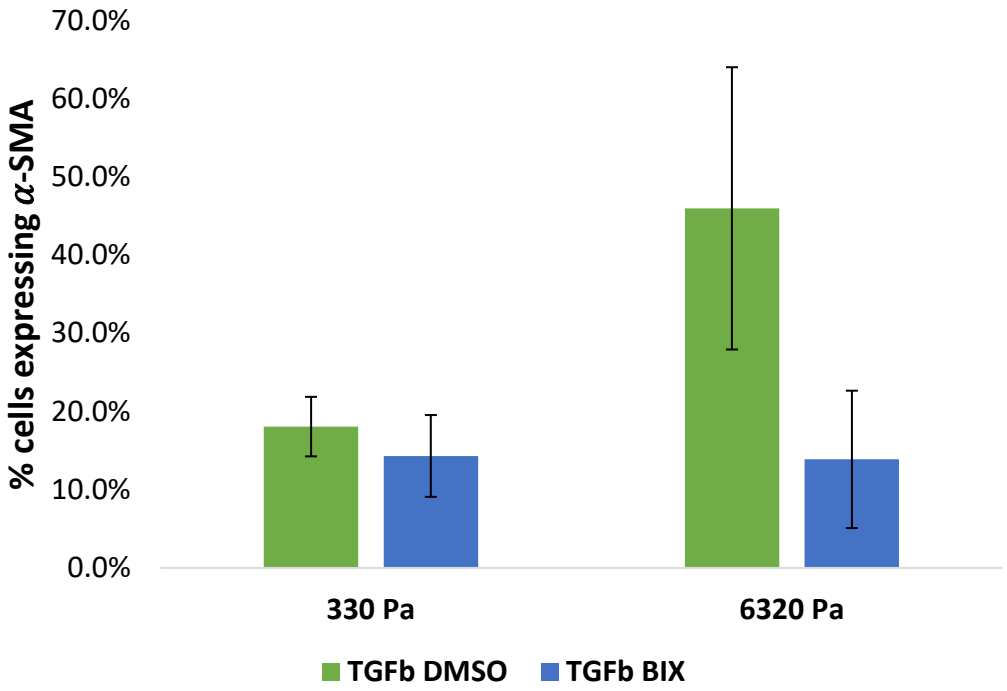

Figure 10: Percentage of TGFβ-treated cells expressing α-SMA on soft (330 Pa) and stiff (6320 Pa) gel substrata

TGFβ-treated cells grown on a stiffer gel matrix (6320 Pa) express α-SMA more frequently than cells grown on a softer gel matrix (330 Pa). Cells treated with BIX express α-SMA less frequently than cells treated with DMSO.

Figure 10 also shows that cells treated with TGFβ and DMSO grown on a stiffer gel matrix (6320 Pa) express α-SMA more frequently than those grown on a softer gel matrix (330 Pa). An increased level of α-SMA indicates that cells grown on stiff substrata mimicking cancerous tissue undergo EMT to a higher degree than cells grown on softer substrata mimicking normal tissue. This result provides more evidence that matrix rigidity has an effect on the extent to which EMT occurs (O'Connor), and it suggests that high matrix rigidity may further induce EMT.

Chapter 4

Conclusions and Future Work

In this thesis, a methodology for characterizing polyacrylamide hydrogels by cavitation rheology began to be developed. A hydrogel composition with known mechanical properties was prepared with two different geometries, and two different equations for determining the elastic modulus were evaluated from the data collected. Equation 2 was found to yield a more accurate Young's modulus, but the data was not reproducible due to issues with the equipment used. For future work on the development of this methodology, additional parts including a camera should be added the experimental setup (shown in Figure 1), which would allow for observation of the cavity within the gel. To further demonstrate that Equation 2 is the appropriate relationship to use for calculating the modulus, the shape of the cavity formed during cavitation should be observed. Additional experiments should also study the effects of needle insertion depth in the material on the calculated modulus.

The other objective of this thesis was to study how extracellular matrix rigidity affects α-SMA expression and TGFβ-induced histone modifications in mammary epithelial cells. The impact of methylation of histones during EMT was studied by treating cells with BIX-01338, a methyltransferase inhibitor. TGFβ-treated cells were found to have lower levels of α-SMA when treated with BIX, suggesting that histone methylation has an effect on EMT. Furthermore, TGFβ-treated cells grown on stiffer substrata were found to have higher levels of α-SMA than those grown on softer substrata, demonstrating that matrix rigidity has an effect on EMT, and suggesting that a higher matrix rigidity may further induce EMT. Future experimentsl should

study how levels of H3K36Me3 change when treated with TGFβ and BIX, and when grown on soft and stiff substrata, to confirm the role of H3K36 during EMT. Additionally, other epithelial and mesenchymal marker levels should be evaluated for cells treated with TGFβ and BIX grown on substrata with different rigidities.

The two projects described in this thesis should be further developed individually. However, in the future they could be combined to study how TGFβ-induced histone modifications are affected when the extracellular matrix undergoes a change in rigidity. A dynamic hydrogel substrate that changes in stiffness over time could mimic the transition between normal and cancerous tissue in the body, and cavitation rheology would allow for the matrix stiffness to be characterized over time without damaging the matrix or the cells growing on it. This and other similar studies would provide more insight into how EMT affects histone modifications. Further understanding of EMT and the factors that affect it can improve our understanding of breast cancer and could perhaps lead to ways to limit or prevent breast cancer metastasis.

REFERENCES

1. National Cancer Institute. Cancer Stat Facts: Female Breast Cancer. https://seer.cancer.gov/statfacts/html/breast.html (accessed Feb 25, 2018).

2. "The basics of epithelial-mesenchymal transition," Kalluri, R.; Weinberg, R.A. *J Clin Invest*, 2009, *119*, 6, 1420-1428.

3. "Epithelial-mesenchymal transition - A fundamental mechanism in cancer progression: An overview," Angadi, P.V.; Kale, A.D. *Indian Journal of Health Sciences*, 2015, *8*, 77-84.

4. "Mechanisms of Disease: epithelial-mesenchymal transition - does cellular plasticity fuel neoplastic progression?" Turley, E.A.; Veiseh, M.; Radisky, D.C.; Bissell, M.J. *Nat Clin Pract Oncol*, 2008, *5*, 280-290.

5. "TGFβ in Cancer," Massague, J. *Cell*, 2008, *134*, 215-230.

6. "Cytoskeletal signaling in TGFβ-induced epithelial-mesenchymal transition," Nalluri, S.M.; O'Connor, J.W.; Gomez, E.W. *Cytoskeleton*, 2015, *72*, 557-569.

7. "Epithelial-mesenchymal transitions in tumor progression," *Nat Rev Cancer*, 2002, *2*, 442-454.

8. "TGFβ-dependent epithelial-mesenchymal transition," Fafet, P.; Vignais M. *Madame Curie Bioscience Database*, 2000.

9. "Genome-scale epigenetic reprogramming during epithelial-to-mesenchymal transition," McDonald, O.G.; Wu, H.; Timp, W.; Doi, A.; Feinberg, A.P. *Nat Struct Mol Biol*, 2011, *18*, 867-876.

10. "G9a is essential for EMT-mediated metastasis and maintenance of cancer stem cell-like characters in head and neck squamous cell carcinoma," Liu, S. et. al. *Oncotarget*, 2015, *6*, 6887-6901.

11. "Remodeling and homeostasis of the extracellular matrix: implications for fibrotic diseases and cancer," Cox, T.R.; Erler, J.T. *Disease Models & Mechanics*, 2011, *4*, 165-178.

12. “Matrix rigidity mediates TGFβ1-induced epithelial-myofibroblast transition by controlling cytoskeletal organization and MRTF-A localization,” O'Connor, J.W.; Riley, P.N.; Nalluri, S.M.; Ashar, P.K.; Gomez, E.W. *J Cell Phys*, 2015, *230*, 1829-1839.

13. “Tissue Cells Feel and Respond to the Stiffness of Their Substrate,” Discher, D.E.; Janmey, P.; Wang, Y. *Science*, 2005, *310*, 1139-1143.

14. “Preparation of Hydrogel Substrates with Tunable Mechanical Properties,” Tse, J.R.; Engler, A.J. *Curr Prot Cell Biol*, 2010.

15. “Cavitation and fracture behavior of polyacrylamide hydrogels,” Kundu, S.; Crosby, A.J. *Soft Matter*, 2009, *5*, 3963-3968.

16. “Soft-solid deformation mechanics at the top of an embedded needle,” Hutchens, S.B.; Crosby,A.J. *Soft Matter*, 2014, *10*, 3679-3684.

17. “Cavitation rheology for soft materials,” Zimberlin, J.A.; Sanabria-DeLong, N.; Tew, G.N.; Crosby, A.J. *Soft Matter*, 2007, *3*, 763-767.

18. “In situ force mapping of mammary gland transformation,” Lopez, J.I.; Kang, I; You, W.K.; McDonald, D.M.; Weaver, V.M. *Integr Biol (Camb)*, 2011, *3*, 910-921.

ACADEMIC VITA

Apoorva Annamraju

apoorva.annamraju14@gmail.com

EDUCATION

Bachelor of Science in Chemical Engineering
Minor in Mathematics
Schreyer Honors College
The Pennsylvania State University, University Park, PA
Anticipated Graduation: May 2018

INDUSTRY EXPERIENCE

Research & Development Intern Summer 2017
Danaher Corporation & Pall Corporation, Pensacola, FL
- Developed post-treatment method for new virus filter membrane
- Coordinated membrane scale-up from laboratory to prototype
- Participated in kaizen to improve process flow in warehouse returns area
- Completed training in continuous improvement and lean manufacturing tools

Global Biotech Operational Excellence Intern Summer 2016
Bayer Pharmaceuticals, Berkeley, CA
- Designed collaboration platforms for project teams using MS SharePoint
- Assisted with lean manufacturing and human performance training programs
- Coordinated site-wide diversity and safety awareness fairs

RESEARCH EXPERIENCE

Undergraduate Research Assistant Fall 2016 – Spring 2018
Esther Gomez Lab, The Pennsylvania State University
- Analyzed epithelial and mesenchymal cell responses to matrix rigidity changes
- Developed cavitation rheology experimental method for research group
- Completed honors thesis on independent research conducted
- Proficient in mammalian cell culturing and fluorescent staining

GLOBAL EXPERIENCE

Mechanical Engineering Product Design Program Summer 2015
National University of Singapore, Singapore
- Designed sustainable product to facilitate cleaning of public spaces in Singapore
- Interacted with Singaporean students and locals to acquire cultural understanding

SOFTWARE & LANGUAGES

Mathematica, Minitab, MS SharePoint, SolidWorks
Proficient in Spanish

LEADERSHIP & INVOLVEMENT

Coach, Penn State Women in Engineering Program Advisory Council (2017-18)
Mentor, Penn State Women in Engineering Program Orientation (2016-17)
Envoy, Penn State Women in Engineering Program Orientation (2016-17)
Chair, Penn State Society of Women Engineers Benefitting THON (2015-16)
Academic Facilitator, Penn State Women in Engineering Program (2015-16)

HONORS & AWARDS

Recipient, Penn State Provost's Award (2014-18)
Recipient, John R. & Jeanette McWhirter Chemical Engineering Fund (2014-18)
Recipient, National Merit Society Corporate Scholarship (2014-18)
Recipient, Penn State President's Freshman Award (2015)